THE JOURNAL OF COMPARATIVE NEUROLOGY 505:221–233 (2007)

Developmental Mechanisms for Retinal Degeneration in the Blind Cavefish *Astyanax mexicanus*

ALESSANDRO ALUNNI,[1] ARNAUD MENUET,[2] EVA CANDAL,[1] JEAN-BAPTISTE PÉNIGAULT,[2] WILLIAM R. JEFFERY,[3] AND SYLVIE RÉTAUX[2]*

[1]MSNC INRA Group, Institut de Neurobiologie Alfred Fessard, Centre National de la Recherche Scientifique, 91198 Gif-sur-Yvette, France

[2]UPR 2197 "Développement, Evolution, Plasticité du Système Nerveux," Institut de Neurobiologie Alfred Fessard, Centre National de la Recherche Scientifique, 91198 Gif-sur-Yvette, France

[3]Department of Biology, University of Maryland, College Park, Maryland 20742

ABSTRACT

The sighted surface-dwelling (surface fish, SF) and the blind cave-living (cavefish, CF) forms of *Astyanax mexicanus* offer a unique opportunity to study the evolutionary changes in developmental mechanisms that lead to retinal degeneration. Previous data have shown the role of increased midline Sonic Hedgehog (Shh) signalling in cavefish eye degeneration (Yamamoto et al. [2004] Nature 431:844–847). Here, we have compared the major steps of eye development in SF and CF between 14 hours and 5 days of development. We have analyzed cell proliferation through PCNA and phospho-histone H3 staining and apoptosis through TUNEL and live LysoTracker analysis. We have assessed the expression of the major eye development signalling factors Shh and Fgf8, and the eye patterning genes *Pax6*, *Lhx2*, *Lhx9*, and *Vax1*, together with the differentiation marker *GAD65*. We show that eye development is retarded in CF and that cell proliferation in CF retina is proportionately similar to SF during early development, yet the retina degenerates after massive apoptosis in the lens and widespread cell death throughout the neuroretina. Moreover, and surprisingly, the signalling, patterning, and differentiation processes leading to the establishment of retinal layers and cell types happen almost normally in CF, although some signs of disorganization, slight heterochronies, and a lack of expression gradients are observable. Our data demonstrate that the evolutionary process of eye degeneration in the blind CF does not occur because of patterning defects of the retina and are consistent with the proposed scenario in which the trigger for eye degeneration in CF is lens apoptosis. J. Comp. Neurol. 505:221–233, 2007.

Indexing terms: evolution; eye; proliferation; cell death; *Shh*; *Fgf8*; *Pax6*; LIM-homeodomain; *Vax1*; GABA; teleost; fish

Vertebrate eyes develop from bilateral evaginations of the anterior neural tube, the optic vesicles. Inside the optic vesicles, the proximal cells form the optic stalk and later differentiate into the glial cells of the optic nerve, whereas distal cells form the two layers of the optic cup and later differentiate into the neural cells and pigment epithelium of the retina. These events are highly dependent on signalling and patterning processes, which are beginning to be understood at the molecular level (for review see Esteve and Bovolenta, 2006). In fish and amphibians, a large fraction of the retinal population is produced by multipotent retinal progenitors in the ciliary marginal zone (CMZ). The CMZ is capable of producing all retinal cell types and allows continuous growth of the retina throughout the life of these animals (for review see Perron and Harris, 2000). Proper eye formation also depends largely on specific and reciprocal interactions between the eye cup and the ectodermal thickening of the

The first two authors contributed equally to this work.

Grant sponsor: Institut de la Génomique Marine and ANR-Neuro, Centre National de la Recherche Scientifique (to S.R.); Grant sponsor: National Institutes of Health; Grant number: EY-14619 (to W.R.J.); Grant sponsor: National Science Foundation; Grant number: IBN-0542384 (to W.R.J.).

*Correspondence to: Dr. Sylvie Rétaux, UPR 2197 "Développement, Evolution, Plasticité du Système Nerveux," Institut de Neurobiologie Alfred Fessard, C.N.R.S., Avenue de la Terrasse, 91198 Gif-sur-Yvette cedex, France. E-mail: sylvie.retaux@iaf.cnrs-gif.fr

Received 2 February 2007; Revised 17 July 2007; Accepted 1 August 2007

DOI 10.1002/cne.21488

Published online in Wiley InterScience (www.interscience.wiley.com).

lens placode: the invagination of this placode forms an open pit, which finally closes in the lens vesicle and whose inner pole cells enlarges and forms the lens fibers (for review see Reza and Yasuda, 2004).

Astyanax mexicanus is a powerful model species in which to study the genetic and developmental mechanisms underlying the evolution of eye degeneration, owing to its two forms: an eyed, surface-dwelling form (surface fish; SF) and several eyeless, cave-dwelling forms (cavefish; CF), which have evolved from an eyed ancestor within the past 1 million years (Mitchell et al., 1971). Although CF initially form eye primordia during embryogenesis, their lens begins to undergo apoptosis at about 25 hours postfertilization (hpf; Jeffery and Martasian, 1998), an event that probably affects the lens signalling to other eye parts (cornea, iris, and retina), which results in the arrest of eye growth, eye degeneration, and sinking of the degenerate eyes into the orbits (Jeffery, 2001). Evidence for the role of the lens in CF eye degeneration has come from transplantation experiments. Indeed, SF eye development is retarded following transplantation of a CF lens into an SF optic cup (Yamamoto and Jeffery, 2000). Conversely, transplantation of an SF lens into a CF optic cup restores eye development. These data indicate that the CF retina conserves the ability to respond to lens signalling and that apoptosis is an autonomous property of the CF lens.

Given the large number of eye markers that are currently known, only a few studies have been concerned with regressive evolution of the CF eye. Among the gene markers that have been studied in the developing retina of the two forms of *Astyanax*, no significant differences have been found, including for major "eye genes" such as *Pax6* (Behrens et al., 1997; Strickler et al., 2001), *Prox1* (Jeffery et al., 2000), *Rx1* and *Vsx2* (Strickler et al., 2002). By contrast, recent evidence for the involvement of Sonic Hedgehog (Shh) signalling at the midline during early embryonic development is available. Indeed, increased midline Shh signalling in CF is responsible for hyperactivation of downstream genes, lens apoptosis, and eye degeneration (Yamamoto et al., 2004). The Shh-driven mechanisms for lens apoptosis are probably indirect and are still to be discovered. Moreover, genetic analyses indicate that multiple genes regulate eye degeneration in CF (Jeffery, 2001; Borowsky and Wilkens, 2002).

Retinal degeneration could be caused either by a decrease in the proliferation rate of the CMZ or by an increase in the rate of programmed cell death. Alternatively, it could result from defects in the patterning mechanisms that govern the development of retinal layers and cell types or even in a loss of ability of cells to differentiate properly. For example, it is known that the outer nuclear layer (ONL) and the photoreceptor layer (among the latest retinal layers to be formed) do not completely differentiate and contain very few photoreceptor cells (Yamamoto and Jeffery, 2000). To gain insights into the molecular events underlying eye degeneration in CF, we have systematically compared proliferation and cell death patterns during development in the eyed SF and in Pachón, one of the CF forms of *Astyanax*. We have investigated whether Shh signalling was modified inside the retina in the same manner as it is at the CF embryonic midline. Additionally, we have examined the expression of factors involved in early eye morphogenesis (*Pax6* and *Fgf8*), in retinal polarity (*Vax1*), or in the patterning or maintenance of neuronal specification and phenotype (*Lhx2*, *Lhx9*, *GAD65*).

Abbreviations

cmz	ciliary marginal zone
di	diencephalon
e	eye
gcl	ganglion cell layer
hyp	hypothalamus
inl	inner nuclear layer
inl_i	inner part of the inl
ipl	inner plexiform layer
le	lens
lep	lens epithelium
nr	neural retina
onl	outer nuclear layer
opl	outer plexiform layer
pi	pigments
rpe	retinal pigment epithelium
tel	telencephalon

MATERIALS AND METHODS

Animals

Laboratory stocks of *A. mexicanus* SF and CF (Pachón population) were obtained from the Jeffery laboratory at the University of Maryland. Fish were maintained at 23–27°C on a 12:12-hour light:dark cycle and treated according the French and European laws on the care and handling of animals in research. Embryos were collected after spawning and fixed at various stages in 4% paraformaldehyde (PFA) diluted in phosphate-buffered saline (PBS). After progressive dehydration in methanol, they were stored at –20°C.

For cyclopamine treatment, 15-hpf embryos were treated for 9 hours in dishes containing 20 μM cyclopamine (Sigma, St. Louis, MO) in water. Control embryos were exposed to 0.1% ethanol, because the cyclopamine stock solution was diluted in 100% ethanol. After treatment, they were washed twice and maintained in fresh water until 48 hpf. They were then fixed and dehydrated for anatomical analysis.

RNA isolation and cDNA cloning

Total RNA from SF brains was reverse transcribed with a random primer using AMV reverse transcriptase (Promega, Madison, WI). Partial or full-length cDNA sequences for *Lhx2* (EF175737), *Lhx9* (EF175738), and *GAD65* (DQ431668) were amplified by PCR with degenerate primers designed after comparing the alignments of several teleost sequences, including zebrafish (Lhx2 forward: 5′-ATGCGIACITCITTYAARCAYCAYCARCT-3′; Lhx2 reverse: 5′-TCAGAAGAGGCTGGTYARRGTG-3′; Lhx9 forward: 5′-ATGCTTTTCCACGGBMTSYC-3′; Lhx9 reverse: 5′-TTAGAAAAGGTTTGTCAAGGTA-3′; GAD65 forward: 5′-CACNCTGAAGAAGATGAGGG-3′; GAD65 reverse: 5′-CCANGCNYCRTCCACRTGCATCC-3′). PCR products were subcloned in TOPO-PCR II vector (Invitrogen, San Diego, CA) and sequenced. *Pax6* (AY651762) and *Vax1* (AY661437) cDNAs were previously isolated by Strickler et al. (2001) and Yamamoto et al. (2004), respectively.

In situ hybridization

cDNAs for genes of interest were amplified by PCR with T7, SP6, or T3 primers, and digoxygenin-labeled ribo-

probes were synthesized from PCR product templates (Nguyen et al., 2001). A protocol for automated whole-mount in situ hybridization (Intavis) was performed as previously described (Deyts et al., 2005). For efficient probe penetration, from 36 hpf, embryos were treated with proteinase K for 30 minutes at 37°C. Several concentrations were used: 10 μg/ml for 36 hpf, 20 μg/ml for 48 hpf, 30 μg/ml for 60 hpf, 40 μg/ml for 72 hpf, and 250 μg/ml for 5–7 dpf. After hybridization, staining was developed with NBT-BCIP solution and embryos were embedded in paraffin and sectioned serially in the transverse plane at 8 μm, or their brains and eyes were dissected out and mounted in glycerol for in toto analysis.

Proliferating cell nuclear antigen, phospho-histone H3, and TUNEL staining

For proliferating cell nuclear antigen (PCNA) immunostaining, embryos were fixed in Clark's solution (3:1 ethanol 100%: acetic acid) overnight at 4°C. They were paraffin-embedded, sectioned as described above, and processed for PCNA immunohistochemistry (monoclonal anti-PCNA ascite fluid, made against a PCNA-protein A fusion protein, which recognizes the acidic, nonhistone, auxiliary protein of DNA polymerase, PCNA, also known as *polymerase delta accessory protein*, from human to yeast; clone PC10 from Sigma; IgG2a isotype, dilution 1/1,000) as previously described (Candal et al., 2005). Phospho-histone H3 immunostaining (rabbit polyclonal IgG anti phospho-H3 (ser10), made against amino acids 7–20 of human histone H3, recognizes a 17-kDa protein on immunoblots and reacts against phospho-histone H3 from *Drosophila* to man (catalog No. 06-570; Upstate Biotechnology/Euromedex; dilution 1/100) and was performed in toto on PFA-fixed embryos and revealed with ABC system (Vectastain Elite ABC kit; Vector, Burlingame, CA). Embryos were then dissected and mounted in toto or dehydrated, paraffin-embedded, and sectioned as described above.

Quantification of Phospho-H3 positive cells at 36 hpf was performed by counting *all* immunopositive cells (including neural retina and lens) on *all* serial sections encompassing the retina from the two eyes of three SF and four CF embryos at 36 hpf. The surface area of the eye in the same collection of serial sections was measured in ImageJ, and the total volume of each eye was then calculated, knowing that the thickness of the paraffin sections is 8 μm. Statistical analyses were performed via two-tailed Student's *t*-test.

Quantification of the cmz volume at 5 dpf was performed by measuring the PCNA-positive area (in ImageJ) on *all* serial sections (8 μm) from the two eyes of one CF and one SF larva. The proliferation zone was then compared with the total volume of the neural retina, also measured with ImageJ on the same serial sections. Quantification of cyclopamine effects on proliferation was performed by counting all phospho-H3-positive cells (including neural retina and lens) on four retina sections from five CF and five SF embryos, chosen in the most central part of the retina (i.e., where the retinal structures are at maximal extension). TUNEL staining was performed using the "In situ Cell Death Detection, POD kit" (Roche), following the manufacturer's instructions.

Lysotracker assay

LysoTracker (Molecular Probes, Eugene, OR) is a vital fluorescent dye that accumulates in acidic intracellular compartments and therefore labels the phagocytosis and autolysis step of apoptosis (for review see Watanabe et al., 2002). Embryos were incubated for 45–60 minutes in LysoTracker-Green (0.05 mM in water), rinsed briefly in fresh water, and mounted alive in water containing MS222 (0.2 mg/ml) for imaging on an Apotome (Zeiss) microscope. All other photographs were taken on a Nikon E800 or a Leica DMP microscope, both equipped with a Nikon Dxm1200 camera. Figures were assembled and images were corrected for cropping, brightness, and contrast in Photoshop CS2.

RESULTS

A. mexicanus is a teleost fish closely related to the well-studied zebrafish. Its development is almost identical to that of zebrafish in the first 48 hpf, so the zebrafish staging table can be used (Kimmel et al., 1995).

Retinal morphogenesis and cell proliferation

We first analyzed the global development and morphogenesis of the retina in *Astyanax* and investigated the possibility that retinal degeneration in CF was due to changes in proliferation patterns. Proliferation has previously been compared at late stages of CF and SF development (10 dpf and 30 dpf), but no differences were reported (Strickler et al., 2002). Thus, here we studied early stages of retinal proliferation by phospho-histone H3 (phospho-H3) and PCNA immunostaining. Phospho-H3 specifically labels cells in M (mitosis) phase of the cell cycle and gives a quantifiable staining pattern, whereas PCNA labels cells in S phase (plus G1 and G2; Fig. 1).

Surface fish. We can distinguish three periods of retina development in SF (Fig. 1). The first period, up to 36 hpf, is characterized by the presence of a proliferating eyefield and eye neuroepithelium, which undergoes classical morphogenetic movements of eye cup formation (Fig. 1A–E). At 36 hpf, the central region of the optic cup is thicker than the peripheral region, but no regional differentiation or layering is appreciable yet (Fig. 1E). The second period of SF retinal development, between 48 hpf and 72 hpf, is characterized by the progressive formation of layers in the central part of the retina. This period begins at 48 hpf with the appearance of a differentiating central region where the inner plexiform layer (IPL) becomes recognizable (Fig. 1F–I). At all subsequent stages, the lateral border of the IPL defines the boundary between the differentiating central retina and the peripheral (proliferating) growth zone, or ciliary marginal zone (CMZ). Pigmentation of the retinal epithelium (outer layer of the optic cup) starts in the central region at about 48 hpf, indicating the beginning of its cytodifferentiation (Fig. 1F). Phospho-H3 and PCNA immunoreactivity (ir) then disappears progressively from the retinal epithelium, following a central-to-peripheral gradient (compare Fig. 1D–G). From 48 hpf onward, the outer nuclear layer (ONL) is clearly distinguished in the most central part of the differentiating retina (Fig. 1F,G). Moreover, the ganglion cell layer (GCL) and numerous cells located in the inner sublayer of the inner nuclear layer (INL_i) are PCNA negative (Fig. 1G). The CMZ and neighboring retina contain exclu-

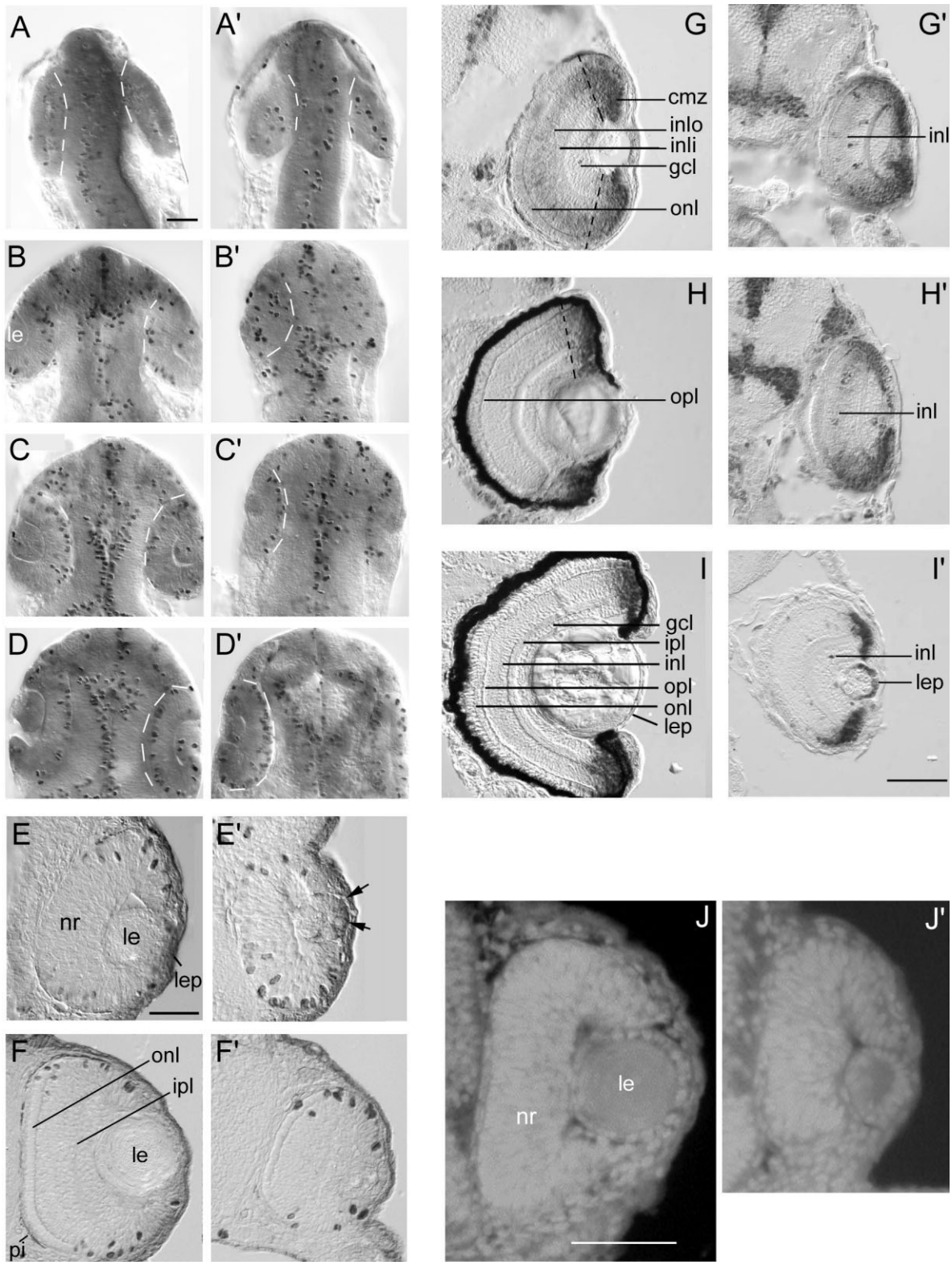

Fig. 1. Proliferation analysis through phospho-histone H3 (A–F′) and PCNA (G–I′) immunohistochemistry in the developing eye of surface fish (**A–J**) and cavefish (**A′–J′**). In toto dorsal views (A–D′; anterior is upward) and transverse sections through the eye (E—J′) of *Astyanax* SF (left) and CF (right) at the following stages of development (hpf, hours postfertilization; dpf, days postfertilization). A,A′: 14 hpf; B,B′: 18 hpf; C,C′: 20 hpf; D,D′: 24 hpf; E,E′: 36 hpf; F,F′: 48 hpf; G,G′: 60 hpf; H,H′: 72 hpf; I,I′: 5 dpf. J,J′ shows DAPI staining at 36 hpf. White dotted lines in A–D′ delineate the optic vesicle. Black dotted lines in G and H delineate the CMZ. For abbreviations see list. Scale bars = 50 μm in A (applies to A–D′); 50 μm in E (applies to E–F′); 50 μm in I′ (applies to G–I′); 50 μm in J (applies to J,J′).

TABLE 1A. Quantification of Proliferation in SF and CF Retina[1]

		Total number of positive cells per eye	Volume of the eye (μm^3)	Density of positive cells per μm^3
Phospho-H3, 36 hpf	SF, n = 6 eyes	385 ± 71	1,362,192 ± 156,416	2.82 10^{-4} cell/μm^3
	CF, n = 8 eyes	206 ± 63	678,368 ± 189,600	3.03 10^{-4} cell/μm^3
		(−46%, $P < 0.05$)	(−50%, $P < 0.02$)	(ns)

[1]At 36 hpf, all phospho-H3-positive cells were counted and the volume of the eyes was calculated. ns, Nonsignificant (Student's *t*-test). See Materials and Methods for details.

TABLE 1B. Quantification of Proliferation in SF and CF Retina[1]

		Volume of the PCNA-positive cmz (μm^3)	Volume of the retina (μm^3)	Percentage of retina volume occupied by the cmz
PCNA, 5 dpf	SF, n = 2 eyes	801,552	5,423,821 (0.005 mm^3)	14.7
	CF, n = 2 eyes	166,616 (−79% vs. SF)	951,232 (−82% vs. SF)	17.5

[1]At 5 dpf, the volume of the PCNA-positive cmz was calculated with regard to the volume of the entire neural retina. ns, Nonsignificant (Student's *t*-test). See Materials and Methods for details.

sively PCNA-ir cells, and these growing borders will remain intensely proliferating throughout development. In the lens and lens epithelium, proliferation progressively decreases as development progresses (see, e.g., Fig. 1D–G). This second period of retinal growth ends at about 72 hpf, when the outer plexiform layer (OPL) becomes clearly distinguishable. From 72 hpf onward, the layers of the retina extend progressively following a central-to-peripheral gradient, characterizing the third period of retinal growth, where the retina essentially consists of a growing CMZ containing PCNA-ir cells and a differentiated, PCNA-negative central retina (Fig. 1H,I).

Cavefish. A significant difference can be noted as early as 14 hpf (Fig. 1A,A′) regarding the size of the CF eye field/eye vesicle/eye cup. The time course analysis shows that CF eye development seems retarded compared with SF (e.g., compare Fig. 1B and C′, C and D′). However, no major proliferation defect is observed in the CF form of *Astyanax* during this first period of retinal growth (14 hpf to 36 hpf): as in SF, the CF retina is an actively proliferating neuroepithelium (Fig. 1A′–E′). This qualitative observation was ascertained by quantification of phospho-H3 staining (Table 1A,B). At 36 hpf, the total volume of the eye (neural retina plus lens) was reduced by 50% in CF compared with SF (Table 1A; see also Fig. 1E,E′); likewise, the total number of phospho-H3 positive cells per eye was reduced by 46% in CF compared with SF (Table 1A). Thus, the average density of proliferating cells was identical in the eyes of the two populations (2.82×10^{-4} phospho-H3 cell/μm^3 in SF vs. 3.03×10^{-4} phospho-H3 cell/μm^3 in CF). Notably, as verified in toto and on sections at various stages, the cellular density appeared similar in the developing eye of the two populations: DAPI staining confirmed the size differences but failed to detect a difference in cell compaction that could underlie the difference of density of proliferating cells reported above (Fig. 1J,J′).

The progressive restriction of proliferation to the CMZ, which is apparent at 36 hpf in SF, is retarded as well in CF (compare Fig. 1E and E′). This retardation in CF eye development continues during the second and third periods defined above. Although both retinal layering and cytodifferentiation begins in 48 hpf SF, these processes are hardly observable in CF at this stage (Fig. 1E′,F′). In 60 hpf CF, as in the SF, the CMZ and the retina neighboring the optic fissure contain only PCNA-ir cells, whereas scattered PCNA-ir cells are also observed the INL. However, in CF, two sublayers (INL_i and INL_o) are not distinguishable (Fig. 1F,G,G′). The proliferation pattern significantly changes in SF between 60 hpf and 72 hpf, but the CF pattern of proliferation remains essentially identical during this developmental period and even more so until 5 dpf (Fig. 1G′–I′). Notably, at 72 hpf, when the SF retina is about twice the size of the CF retina, their proliferative areas are comparable in size (Fig. 1H,H′). This is even more striking at 5 dpf, when the SF retina is five times larger than its CF counterpart (Table 1B) but when the proliferating CMZ is still very active (Fig. 1I,I′) and occupies an equivalent portion of the retina volume as in its SF counterpart (Table 1B). Proportionately, the dying CF retina proliferates as much as the growing and healthy SF retina. In the CF form, proliferation in the lens epithelium is also maintained until 5 days of development (Fig. 1I′), whereas, at these same stages (48 hpf), Yamamoto and Jeffery (2000) have shown that the lens is dying by apoptosis (see also below).

Because the reduction of eye size in CF probably is due to increased Shh midline signalling during early development and subsequent reduction of the *Pax6* eye field domain (Strickler et al., 2001; Yamamoto et al., 2004), we next investigated whether increased Shh in CF was also responsible for maintaining sustained proliferation in the retina. Quantification of phospho-H3 positive cells in the retina of 48 hpf CF embryos that had been treated with 20 μM cyclopamine (cyclopamine is a potent inhibitor of Shh signalling through binding to its receptor Smoothened; see Menuet et al., 2007) between 15 hpf and 24 hpf demonstrated that proliferation in CF retina was not dependent on Shh signalling during this developmental window (data not shown).

Programmed cell death

CF retinal degeneration is apparently not caused by decreased proliferation, so we next compared the pattern of cell death by TUNEL labelling on sections from SF and CF. Previous analysis has shown massive apoptosis in the lens of CF, starting at 25 hpf (Jeffery and Martasian, 1998) and still present at 5 dpf and 10 dpf (Soares et al., 2004), which appears to be Shh dependent (Yamamoto et al., 2004). Here, we investigated and compared apoptosis in sections of the neural retina through earlier development (Fig. 2).

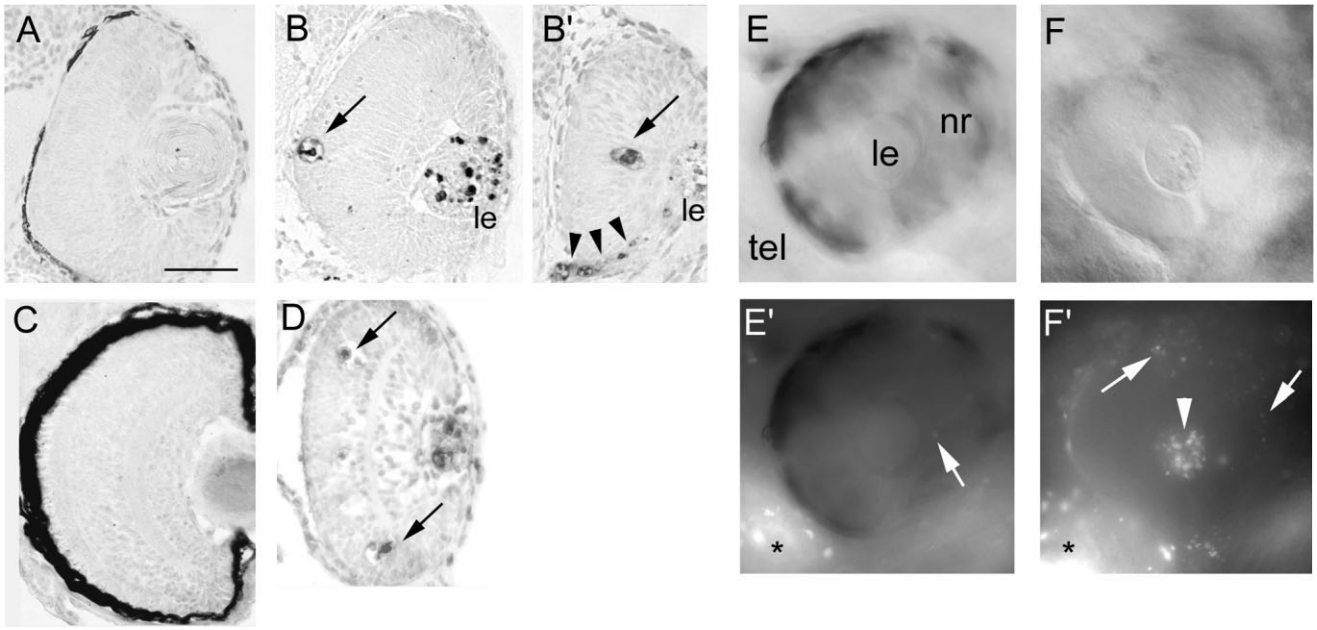

Fig. 2. Analysis of apoptosis through TUNEL labelling (**A–D**) and live imaging using LysoTracker-Green (**E–F′**). TUNEL labelling is shown at 48 hpf (A–B′) and 72 hpf (C,D) in surface fish (A,C) and cavefish eye sections (B,B′,D). Arrows in B, B′, and D indicate hot spots of apoptosis in the neural retina. In B′, arrowheads indicate apoptosis along the optic nerve. LysoTracker-loaded surface fish (E,E′) and cavefish (F,F′) embryos were photographed at 40 hpf under Nomarski optics (E,F) and fluorescence (E′,F′), with anterior to the left and dorsal upward. In E′,F′, arrows point to cell death in the retina, arrowheads indicate cell death in the lens, and asterisks indicate important cell death reproducibly found in all embryos in the telencephalon, which can serve as an internal control. For abbreviations see list. Scale bar = 50 μm.

No cell death can be detected with the TUNEL method in SF at the studied stages (Fig. 2A,C). By contrast, apoptotic cells are present in the CF retina (Fig. 2B,B′,D). These dying cells are observed primarily and are most numerous in the lens, but are also observed throughout the neural retina, starting at about 48 hpf, in cells apparently randomly located throughout the retinal layers. TUNEL-positive cells were often observed as groups of cells, which are suggestive of "hot spots" of cell death. Moreover, in some cases, massive apoptosis was also observed along the optic nerve exit (Fig. 2B′).

The amount of programmed cell death detected by TUNEL was relatively low to account for SF/CF difference in eye size and for CF eye degeneration process, so we sought to analyze cell death with another, more sensitive marker. To this end, we used the fluorescent probe LysoTracker (LT), which labels acidic organelles in living cells, to detect apoptotic cell death on live embryos (see Materials and Methods). With this marker, two independent experiments showed that CF eyes (n = 16) presented a very strongly labeled lens (almost completely labeled; Fig. 2F′) and numerous LT-positive cells dispersed through the retina (Fig. 2F′), whereas SF eyes (n = 15) had LT-negative lens and occasionally presented one or two LT-positive cells in the retina in the plane of the photography (Fig. 2E′). Thus, these live imaging experiments were able to detect significant and early (from 35 hpf, not shown) degenerating process in the CF neural retina.

Signalling pathways

Shh. Because Shh expression is up-regulated all along the midline of CF embryos (Yamamoto et al., 2004), because this increased Shh signalling is, indirectly, responsible for retinal degeneration, and because Shh has important functions in regulating cell cycle exit and differentiation inside the retina (Levine et al., 1997; Stenkamp et al., 2000; Shkumatava et al., 2004; Moshiri et al., 2005; Shkumatava and Neumann, 2005; Wang et al., 2005), we compared Shh expression in SF and CF developing eye (Fig. 3A,B). At 48 hpf in SF and CF, *Shh* mRNA is expressed in the GCL, with a relatively higher expression in the center of the retina, but not in other cell layers nor in the CMZ; *Shh* is not expressed in the lens but is also consistently expressed in the retinal pigment epithelium (nonpigmented in the case of CF). No significant difference between SF and CF could be detected either in the pattern or in the intensity of *Shh* expression (Fig. 3A,B). Identical results were found at 60 hpf (data not shown).

Fgf8. Fgf8 has recently been postulated as a local retina organizing center that initiates retinal differentiation (Martinez-Morales et al., 2005) and axial patterning of the retina (Picker and Brand, 2005). Martinez-Morales et al. (2005) also found that this Fgf8 signalling center is localized in a species-specific manner. In *Astyanax*, *Fgf8* is expressed in the most central part of the CMZ at 48 hpf (Fig. 3C,D). As for the Shh signalling system, no significant differences are observed with respect to *Fgf8* mRNA expression between SF and CF populations (identical results at 60 hpf; data not shown).

Homeodomain-containing patterning factors

Pax6. Because Pax6 has been shown to be indispensable for the development of various retinal cells and plays important roles in lens development (see the introductory

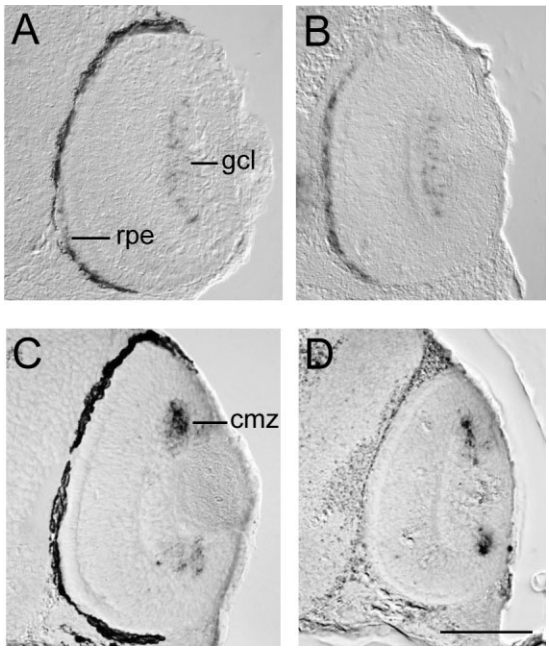

Fig. 3. Expression of *Shh* (**A,B**) and *Fgf8* (**C,D**) mRNA in the developing eye of surface fish (left, A,C) and cavefish (right, B,D) at 48 hpf. For abbreviations see list. Scale bar = 50 μm.

paragraphs), we analyzed its expression pattern during SF and CF development.

Surface fish. In 36 hpf SF, *Pax6* mRNA is observed throughout the lens and in the prospective GCL and INL (Fig. 4A). As development proceeds (in 48 hpf SF), *Pax6* expression increases in the CMZ, the GCL, and the inner part of the INL (INL_i); conversely, it decreases in lens, except in the lens epithelium (Fig. 4C). In 60 hpf SF, *Pax6* mRNA expression is detected in the CMZ and INL_i, whereas it decreases in the GCL and lens epithelium (Fig. 4E).

Cavefish. In 36 hpf CF, *Pax6* mRNA expression is observed throughout the lens and in the prospective GCL and INL of the immature, disorganized, and pseudostratified retina, although the relative number of Pax6-expressing cells is clearly higher than in SF (Fig. 4A,B). Increasing numbers of *Pax6*-positive cells are observed in 48 hpf CF (Fig. 4D). Unlike the SF form, the number of *Pax6*-expressing cells does not decrease in 60 hpf CF, where they are observed throughout the GCL, INL_i, radial "ectopic" columns in the INL_o, and even the ONL. They are also observed in the lens epithelium (Fig. 4F).

Lhx2 and Lhx9. *Lhx2* and *Lhx9* are two paralog members of the LIM-homeodomain transcription factor family. Lhx2, which is part of the genetic network for vertebrate eye development (Zuber et al., 2003), is supposed to have a role in the control of proliferation in the forebrain (Por-

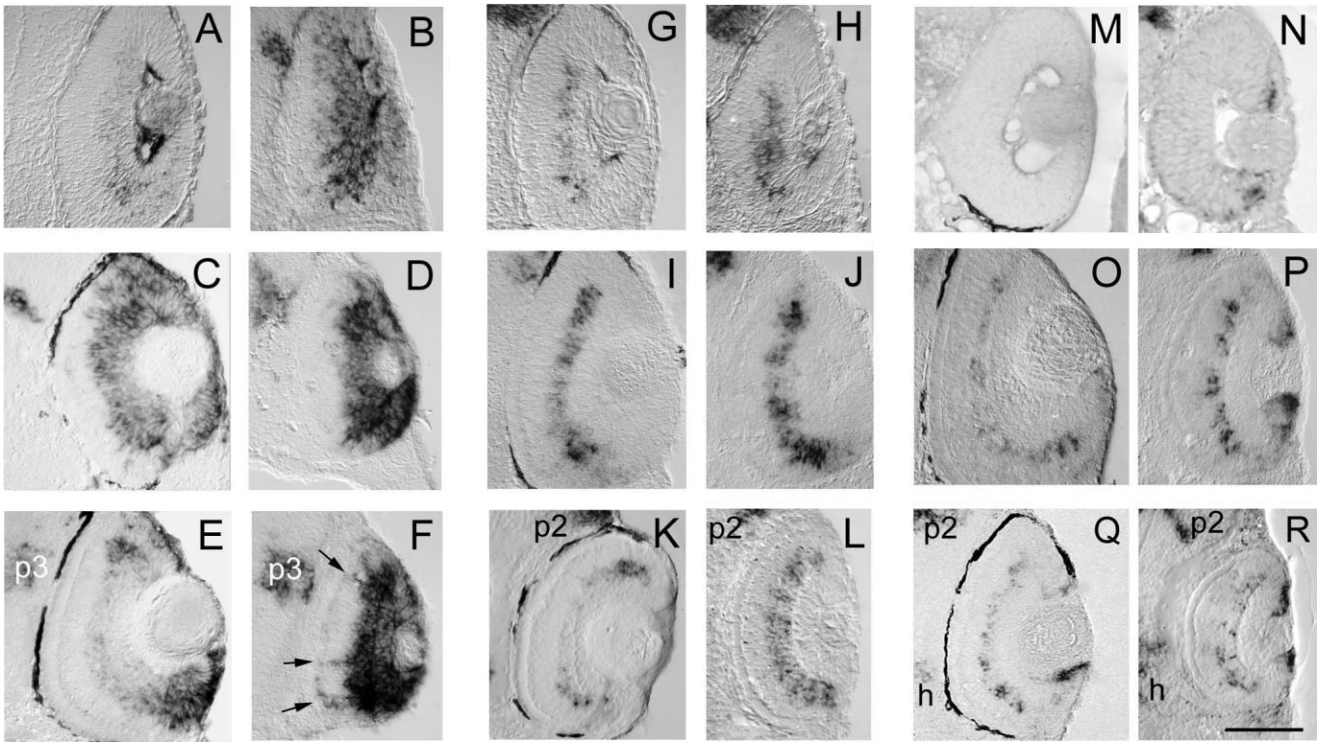

Fig. 4. Expression of *Pax6* (**A–F**), *Lhx9* (**G–L**), and *Lhx2* (**M–R**) mRNA in the developing eye of surface fish (A,C,E–G,I,K–M,O,Q) and cavefish (B,D,F–H,J,L–N,P,R) at 36 hpf (A,B–G,H–M,N), 48 hpf (C,D–I,J–O,P), and 60 hpf (E,F–K,L–Q,R). In the *Pax6* panel (F), arrowheads point to "ectopic" columns of *Pax6*-positive cells extending into the outer nuclear layer. Note that, for this and following figures, we do not consider the staining intensity of the ISH, which is not a quantitative method, but exclusively differences in pattern (gradients, absence or presence of expression, shape or extension of an expression domain). Also note that the studied genes are also expressed in the brain, which can be taken as an "internal control" of ISH. As indicated for stage 60 hpf, expression of *Pax6* in prosomere 3 (p3) and *Lhx2/Lhx9* in prosomere 2 (p2) and hypothalamus (h) is identical in both populations. For abbreviations see list. Scale bar = 50 μm.

ter et al., 1997; Ando et al., 2005). *Lhx2*$^{-/-}$ mice are eyeless (Porter et al., 1997). On the other hand, nothing is known of the role or expression of *Lhx9* during eye development. Here, we describe similar but distinct cellular expression of the two LIM-hd paralogs in the *Astyanax* retina as well as differences in expression between CF and SF forms.

***Lhx2*.**

Surface fish. *Lhx2* is not expressed in the 24 hpf or 36 hpf SF retina (Fig. 4M). One day later, in 48 hpf SF, a discontinuous, patchy, *Lhx2* mRNA expression is observed in the INL_i, and a few cells are labelled in the CMZ (Fig. 4O). In 60 hpf SF, gaps of *Lhx2* expression are still observed in the most central part of the INL; notably, *Lhx2* expression in the CMZ is stronger than at earlier stages and appears in its most marginal part, i.e., in a pattern that appears complementary to that of *Fgf8* (compare Figs. 4Q and 3C).

Cavefish. In contrast to the case in SF, *Lhx2* expression in CF is already detectable at 36 hpf at the margin of the retina (Fig. 4N). In 48 hpf CF, the global *Lhx2* pattern is comparable to that of SF (discontinuous expression in the INL_i), but the relative number of *Lhx2*-expressing cells in the CMZ is higher than in SF, particularly in its most marginal part (Fig. 4P). In contrast to the case in SF, *Lhx2*-expressing cells are still numerous in the most central retina of 60 hpf CF and reflect a relative disorganization of the CF retina (Fig. 4R). CMZ *Lhx2* expression continues to be much greater in CF than in SF at 60 hpf.

Lhx2 is the only marker we have found to be expressed earlier in CF retina. It is expressed in the CMZ and has a suspected role in proliferation (see Discussion). We thus tested whether cyclopamine treatment in CF would delay its onset of expression in the CMZ. At 36 hpf, *Lhx2* was already strongly expressed in the CMZ of treated embryos (n = 11/11; data not shown), indicating that its early onset in CF is not dependent on Shh signalling between 15 hpf and 24 hpf and reinforcing the results found with cyclopamine treatment on proliferation experiments.

***Lhx9*.**

Surface fish. Like *Lhx2*, *Lhx9* is not expressed in the *Astyanax* retina at 24 hpf (not shown). Starting at 36 hpf, *Lhx9* mRNA expression is observed bordering the future CMZ. Since all cells at this stage are PCNA-ir, *Lhx9* could specify the limits of the future differentiation zones. *Lhx9* expression is also detected in the INL_i (Fig. 4G), in a region that is free of mitotic (phospho-H3 positive) cells. In 48 hpf SF, a homogeneous *Lhx9* expression is observed in the INL_i, which is absent from the CMZ (Fig. 4I). In 60 hpf fishes, *Lhx9* expression is strongly decreased in the most differentiated central INL_i (almost absent), although it keeps bordering the CMZ (Fig. 4K).

Cavefish. In 36 hpf CF, as in SF, *Lhx9* borders the future CMZ and is also observed in the INL, where it labels a seemingly broader "layer," probably reflecting the disorganization of the CF retina (Fig. 4H). At 48 hpf, a discontinuous, again relatively disorganized expression of *Lhx9* is observed in the INL_i, although this gene marker is now absent from the CMZ (Fig. 4J). At 60 hpf, *Lhx9* expression is not down-regulated in the CF central retina and is therefore similar to that observed in the SF form at previous developmental stages (48 hpf); that is, a homogeneous expression is observed in the INL, and expression is absent from the CMZ.

***Vax1*.** Vertebrate *Vax* genes (*Vax1* and *Vax2*) are *Emx*-related homeodomain containing genes that are implicated in the dorsoventral patterning of the neural retina (Barbieri et al., 1999; Schulte et al., 1999), the development of the optic stalk, and the closure of the choroid fissure (Barbieri et al., 1999; Take-uchi et al., 2003). Their expression is regulated by Shh, and possibly Fgf, signals (Take-uchi et al., 2003). We thus analyzed the distribution of one of these genes in the two forms of *Astyanax* (Fig. 5).

Surface fish. At 24 hpf, *Vax1* is expressed as a ventral belt at the diencephalic level: a continuous band of expression is observed in the ventral diencephalon and the optic stalks (Fig. 5A,B), as in zebrafish (Take-uchi et al., 2003). At 36 hpf, 48 hpf, and 60 hpf, *Vax1* expression is still readily detected in the ventral diencephalon. Moreover, in the eye, *Vax1* is confined to the ventral retina and is progressively restricted to the ventral CMZ, with occasional faint labelling in the ventral aspect of the INL (Fig. 5B–D).

Cavefish. At 24 hpf, and as has already been shown to be a consequence of increased midline Shh signalling by Yamamoto et al. (2004), CF diencephalic *Vax1* expression is expanded compared with SF (Fig. 5E). At 36 hpf, the expansion of the *Vax1* domain, although present, is less prominent (Fig. 5F), and its expression in the ventral retina becomes comparable to that in SF embryos. By 48 hpf, although diencephalic *Vax1* expression is still strong (asterisk in Fig. 5G) and slightly expanded compared with SF (not shown), the CF retina has down-regulated this marker in its ventral region (Fig. 5G). Finally, at 60 hpf, *Vax1* is no longer expressed in the CF ventral retina, although strong hybridization signals can still be readily detected in the diencephalon (asterisks in Fig. 5H).

A terminal differentiation marker: GAD65

γ-Aminobutyric acid (GABA) is a major inhibitory transmitter of the teleost retina (Marc and Cameron, 2001; Yazulla and Studholme, 2001). Glutamic acid decarboxylase (GAD65) is one of the two rate-limiting enzymes for GABA biosynthesis and can therefore be used as a marker for differentiated, GABAergic neurons. In both SF and CF forms of *Astyanax*, the expression of *GAD65* mRNA is first detected at about 48 hpf.

***Surface fish*.** In 48 hpf fishes, *GAD65* mRNA expression is observed in the INL_i. This expression is particularly concentrated in the central retina and rather diffuse to the periphery, i.e., follows the expected differentiation gradient (Fig. 6A). *GAD65* expression remains similar in 60 hpf embryos. In both 48 hpf and 60 hpf embryos, a weak ventral-high to dorsal-low gradient of *GAD65* expression is reproducibly found in the SF retina (Fig. 6A,C).

***Cavefish*.** In 48 hpf and 60 hpf CF, *GAD65* expression is homogeneously observed in the INL_i, in a relatively larger "layer" than in SF (Fig. 6B,D), a finding comparable to what has been found for *Lhx9* (see Fig. 4I,J). Moreover, CF eyes do not present any ventrodorsal gradient of *GAD65* expression, a result that is therefore parallel to the absence of ventralizing *Vax1* factor in the CF retina (Fig. 5H).

DISCUSSION

To understand better the molecular and cellular mechanisms involved in CF eye development and degeneration, we have systematically compared cell proliferation, cell death, signalling molecules, and genetic specification in the retina of Pachón CF and their surface counterparts.

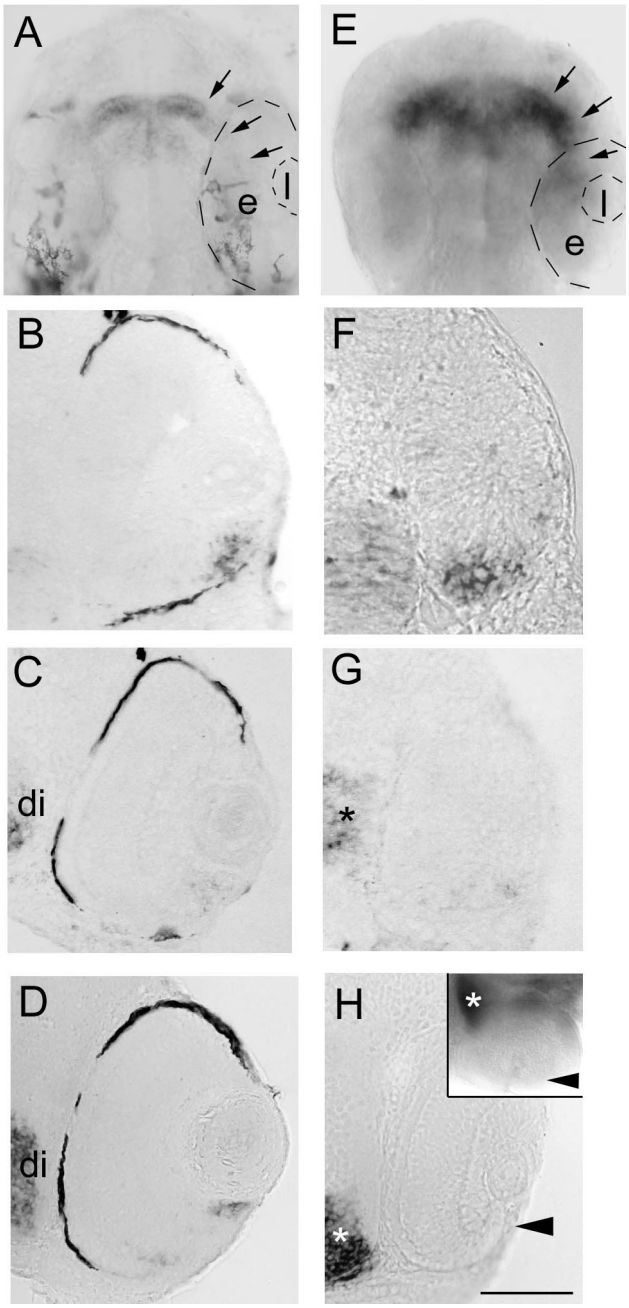

Fig. 5. Expression of *Vax1* mRNA in the developing eye of surface fish (left, **A–D**) and cavefish (right, **E–H**). Stages are as follows: A,E: 24 hpf; B,F: 36 hpf; C,G: 48 hpf; D,H: 60 hpf. A,E show in toto ventral views, whereas B–H show transverse sections through the eye. The **inset** in H is an in toto lateral view of a 60-hpf embryo, showing the absence of *Vax1* mRNA in the retina, whereas the diencephalon behind exhibits strong expression. The arrowheads point to the absence of *Vax1* signal in the ventral CMZ of cavefish, whereas the asterisks indicate strong labelling in the diencephalon. Dashed lines in A and E delineate the eyes. For abbreviations see list. Scale bar = 50 μm.

We found that CF eyes show surprisingly correct proliferation, patterning, and differentiation processes and that they begin to degenerate by apoptosis in the lens at 24 hpf and in the neural retina at about 35 hpf (Fig. 7).

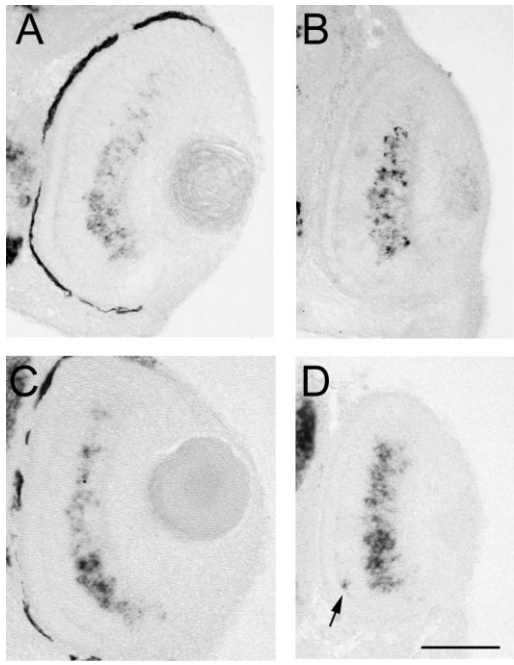

Fig. 6. Expression of *GAD65* mRNA in the developing eye of surface fish (**A,C**) and cavefish (**B,D**) at 48 hpf (A,B) and 60 hpf (C,D). The arrow in D points to an "ectopic" *GAD65*-positive cell in the ONL. For abbreviations see list. Scale bar = 50 μm.

Proliferation and apoptosis patterns

In fish and amphibians, a large fraction of retinal neural cells is produced by progenitors of the CMZ (for review see Harris and Perron, 1998; Perron and Harris, 2000). In addition, slowly dividing cells are continuously born in the INL and then migrate into the ONL (Faillace et al., 2002). Such a pattern has been found in several fishes, including zebrafish and trout (Marcus et al., 1999; Candal et al., 2005), and in the eyed surface form of *Astyanax* (present results). Here, we show that an active CMZ is also present in CF, suggesting that CF retina regression is not due to an early proliferation defect. At later stages of development (10 dpf to 30 dpf), Strickler and colleagues (2002) have shown that the CMZ progeny incorporate normally in the central retina of CF. The results of both studies suggest that the CF retina may attempt to compensate for small size and for defective signalling from the lens and/or for cell death by maintaining a very active and large CMZ in proportion to its overall size (see Fig. 1). In addition, the CF retina has numerous "ectopic" PCNA-positive or phospho-H3 cells in all layers of the central retina, even at late stages (5 dfp). Moreover, quantification of phospho-H3-positive cells indicates that the proliferation rate is proportionately similar in the CF and SF eyes. Increases in the normal rate of proliferating cells in the INL have been found after injury in teleost fishes, when a part of the retina activates mitotic activity of proliferating cells in the INL near and far from the lesion (Faillace et al., 2002). Thus, the presence of numerous proliferating cells in the central retina of CF can be viewed as a sign of retinal stress.

Similar conclusions can be drawn concerning lens proliferation. Both in SF and in CF, the lens epithelium

proliferates continuously; its posterior cells exit the cell cycle and transform into primary fibers in the case of SF or undergo massive cell death in the case of CF (for a recent review on lens development see Reza and Yasuda, 2004). Thus, the degenerating CF lens epithelium proliferates normally, and lens degeneration seems to be due exclusively to apoptosis of fiber cells. Recent data suggest that the heat shock protein chaperone hsp90α has a role in this process, although it remains unclear how lens apoptosis is initiated by this molecule (Hooven et al., 2004).

We have confirmed and imaged in live embryos that lens apoptosis, which starts at 25 hpf (Jeffery and Martasian, 1998), is continuous and massive through embryonic stages. It has been previously shown that this event is causal in CF eye degeneration (Yamamoto and Jeffery, 2000). In addition, we describe significant cell death inside the neural retina, starting at about 35 hpf. There, the few "hot spots" of apoptotic cells observed by TUNEL could not account for the size reduction of the CF retina compared with SF (which can already be observed as early as 14 hpf, i.e., long before the onset of apoptosis). This led us to analyze cell death in live animals using LysoTracker, a fluorescence-labelled probe which accumulates in acidic cellular compartments. This method allowed the detection of earlier and greater cell death in the neuroretina than when measured with the TUNEL method. A higher sensitivity of the LT method was similarly reported in other developmental systems, such as heart morphogenesis (Schaefer et al., 2004), and is attributed to the fact that LT detects apoptotic bodies whether they have fragmented DNA or not, whereas TUNEL detects only apoptotic bodies with concentrated DNA fragments (Watanabe et al., 2002; Schaefer et al., 2004). The possibility that LT detects other forms of cell death (necrosis, autophagy) still remains, but the same holds true for TUNEL (Watanabe et al., 2002). With respect to the CF retina, our results indicate significant apoptosis in the neural retina as early as 35 hpf and suggest that apoptotic cells are probably rapidly removed.

Shh and neurogenesis

In fish and amphibians, CMZ progenitors differentiate into all retinal types, which incorporate seamlessly into the retina as the eye grows. A CMZ has also been demonstrated in chick, although it is not capable of differentiating into all cell types (Fisher and Reh, 2000; Reh and Fisher, 2001). Neurogenesis occurs in several waves, and progenitors depend on Shh as a proliferative signal both during embryonic development and at the CMZ after hatching (Moshiri et al., 2005). Shh is able to bias CMZ progenitor cells toward retinal ganglion cells (RGC): the first neurons to be born in the first wave of differentiation in the retina are the RGC, and they express Shh (Shkumatava et al., 2004; Moshiri et al., 2005; Cheng et al., 2006). Shh produced by differentiated RGC maintains the proliferation of the progenitor cells localized ahead of the wave front and thus is thought to propagate the wave of RGC genesis (Neumann and Nuesslein-Volhard, 2000). A second wave generates amacrine cells expressing Shh and overlaps with the first RGC wave, but does not depend on it, insofar as it occurs in the absence of RGC (Shkumatava et al., 2004). Another, distinct wave of Shh expression occurs in the retinal pigmented epithelium and seems responsible for the propagation of photoreceptor differentiation in the ONL (Levine et al., 1997; Stenkamp et al., 2000).

Because a modification of Shh along the cavefish embryonic midline at neural plate stage is (indirectly) responsible for lens apoptosis and eye degeneration (Yamamoto et al., 2004), we sought to analyze Shh expression in the retina. We observed in *Astyanax* the two "waves" of Shh retinal expression in the RGC and the RPE, both in SF and in CF. Hence, the first wave of neurogenesis that allows differentiation of RGC seems to occur normally. The formation of an IPL in the 48 hpf CF (which coincides with the formation of the same layer in the SF) supports this idea, because RGC have a role in organizing the presynaptic inputs, and the formation of the IPL is delayed when ganglion cells are never born (Kay et al., 2004). In addition, we observed the formation of an INL in both CF and SF, suggesting that the second wave of neurogenesis, which gives rise to amacrine cells, also happens normally in CF. Finally, we observed identical expression of Shh in CF and SF retina "pigment" epithelium (unpigmented in the case of CF). Thus, the photoreceptor differentiation defect described in CF (Langecker et al., 1993; Yamamoto and Jeffery, 2004) does not occur through modified Shh signalling. As a whole, it is therefore very unlikely that a modification of Shh signalling locally inside the CF retina is responsible for differentiation defects and cell death. We can further conclude that the up-regulation of Shh previously observed at the embryonic midline (Yamamoto et al., 2004) is not observed in the retina, an observation that suggests that regulation of Shh expression in the CNS midline and in the bilaterally developing retina are distinct. Finally, we can deduce from cyclopamine treatments that increase in midline signalling during eye development (between 15 hpf and 24 hpf) is not responsible for sustained proliferation in their eyes, a phenomenon that can rather be viewed either as a compensation mechanism due to retinal stress or as an attempt to recover from developmental delay and to regulate eye size.

Shh stimulates proliferation of CMZ progenitors of posthatching animals in vivo (Moshiri et al., 2005), and changes in the Shh signalling system may be involved in the reduction in postembryonic retinal growth of mammals. However, a reduction of *Shh* expression is not observed in CF. Although *Shh* mRNA expression should not be taken as an index of Shh signalling, our data nevertheless suggest that the neurogenic waves occur normally, and that reduced size and degeneration are a secondary phenomenon during CF retina development. This conclusion is also supported by the globally highly similar expression patterns of retinal transcription and differentiation factors we observed in CF compared with SF.

Pax6

Seemingly divergent conclusions have been proposed for the involvement of *Pax6* in the evolution of CF eye regression. Using radioactive in situ hybridization, Behrens et al. (1997) have found no difference in pattern, strength, or time course of *Pax6* mRNA expression between the surface form and the Piedras CF of *Astyanax*. Conversely, using Pax6 immunohistochemistry, Strickler et al. (2001) have found slight differences in the lens and the corneal epithelium of Pachón CF compared with SF, which, together with their major finding on early neurula differences of *Pax6* expression at the anterior midline, led them to suggest that changes in *Pax6* expression are involved in

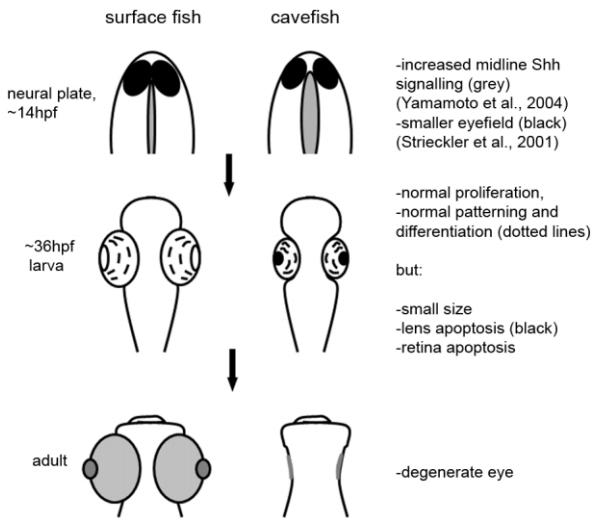

Fig. 7. Comparison of SF and CF development, showing the successive events leading to eye degeneration in CF. See text for details.

the evolution of CF eye regression. Here, we used nonradioactive in situ hybridization for *Pax6* mRNA. As with all other markers used, we do not consider differences of intensities of the hybridization signal but only differences in pattern (gradient, absence or presence, shape and extension of a domain). Although the major features of *Pax6* expression are similar between CF and SF, in that both forms show labelling in the lens (at 36 hpf) and lens epithelium (at later stages), and, for the CMZ, GCL, and INL, we observe 1) a wider expression and 2) a disorganization of *Pax6* expression throughout the eye. We suggest that the discrepancies in previous investigations are due mainly to the techniques employed, to the ages of the embryos, and/or to the form of CF used. Our results favor an involvement of *Pax6* in eye degeneration in Pachón CF, but the type of expression changes we observe in their eyes cannot discriminate between a scenario in which *Pax6* up-regulation is a consequence of retinal degeneration and a scenario in which *Pax6* change is causal in retinal degeneration (see also below).

Patterning and differentiation

We have isolated and used three markers that label the differentiating and/or differentiated INL: *Lhx2*, *Lhx9*, and *GAD65*. Consistent with a role of the two LIM-hd factors in neuronal differentiation, their expression in the central retina appears after 36 hpf (*Lhx9*) or after 48 hpf (*Lhx2*), when the first waves of neurogenesis concerning the ganglion cells and the INL arise. Similarly, the GABA biosynthesis enzyme is first detected at stage 48 hpf in the INL, a labelling that probably corresponds to the GABAergic amacrine cells. As noted above, there are no gross patterning defects in the CF retina compared with its SF counterpart. The layer of *Lhx2*/*Lhx9*/*GAD*-expressing cells is slightly larger in the CF retina; a slight (but probably important) heterochrony in the expression patterns is sometimes detected (*Lhx9* in CF at 60 hpf is very similar to the SF 48 hpf pattern; *Lhx2* onset of expression is earlier in CF); and some signs of disorganization can be observed (e.g., *Lhx2*/*Lhx9* patches or columns of cells or "ectopic" *GAD65* in CF). However, the patterning processes appear to occur in a remarkably normal fashion, and, apart from its small size, the CF neural retina develops according to a normal program. This probably explains how lens transplantation from a SF into a CF embryo is able to rescue CF eye development (Yamamoto and Jeffery, 2000): before cells of the central retina start dying at about 35 hpf, the CF neural retina is healthy and develops normally, despite its small size.

Lhx2 is one of the six known "eye field transcription factors" that can induce ectopic eyes in *Xenopus* (Zuber et al., 2003). It has recently been isolated in zebrafish as the gene affected in the *belladonnal* (*bel*) mutant (Seth et al., 2006). In contrast to the *Lhx2*$^{-/-}$ mice, which are eyeless (Porter et al., 1997), *bel* zebrafish do have eyes, although they lack most amacrine cells and are small and disorganized (Seth et al., 2006). Our observation in *Astyanax* of *Lhx2* expression in the INL is consistent with these recent findings. We have also observed that *Lhx2* is expressed in the proliferating CMZ and that the onset of this expression is delayed in time in SF compared with CF. Insofar as a general role for *Lhx2* in the positive control of proliferation in the nervous system is strongly suspected (Porter et al., 1997; Ando et al., 2005; Seth et al., 2006), and insofar as proliferation markers indicate that the CF eye proportionately proliferate as much as the SF eyes, it may be relevant to interpret the advanced onset of *Lhx2* expression in CF as an attempt to compensate for the ongoing process of degeneration. The absence of effect of cyclopamine treatment on the onset of Lhx2 expression in CF is in favor of this hypothesis; it parallels the similar lack of effect found on phospho-H3 proliferation pattern.

Retinal polarity

Axial eye patterning determines the positional code of RGCs, which is crucial for the establishment of the topographic representation of retinal inputs onto the optic tectum (for reviews see Retaux and Harris, 1996; Goodhill and Richards, 1999; Lemke and Reber, 2005). *Vax* genes probably play a key role in this process. They ventralize the embryonic eyes (Barbieri et al., 1999; Mui et al., 2005), and they are induced by Shh (Take-uchi et al., 2003). One difference we have found between CF and SF retinas concerns *Vax1* expression. Whereas *Vax1* is expanded at early stages in CF, it is notably absent from the ventral retina of CF at late stages of development. This is one of the few examples of a gene down-regulated in CF; most developmental patterning genes previously studied seem to be up-regulated in CF (Yamamoto et al., 2004; Menuet et al., 2007). Moreover, the absence of the ventralizing *Vax1* factor is accompanied by the absence of a *GAD65* gradient in the CF neural retina, again indicating a dorsoventral polarity defect in the CF eye. A transient retinotectal projection does develop in CF, although it is reduced and unresponsive to light stimuli (Voneida and Sligar, 1976; Soares et al., 2004). It would therefore be interesting to investigate whether this projection is devoid of any topographical organization.

Fgf8 was recently demonstrated to signal nasotemporal axial patterning in zebrafish (Picker and Brand, 2005). On the other hand, dorsoventral eye patterning involves Bmp4, which is expressed in the dorsal region of the eye and leads to up-regulation of the dorsal factor *Tbx5* and to down-regulation of the ventral factors *Vax* and *Pax2* upon misexpression (Koshiba-Takeuchi et al., 2000; Sasagawa

et al., 2002). As confirmed by our cyclopamine experiments (not shown), midline-derived Shh is responsible for *Vax* regulation and diencephalic patterning, and recent results have suggested a collaboration of retinoic acid and Fgfs with Shh for the ventralization of the eye (Lupo et al., 2005). Thus, the ventralization defect we observe here in CF eyes that do not express *Vax1* in the correct place and time is probably a consequence of the changes in midline signalling previously described in CF (Yamamoto et al., 2004) and further exemplifies the role of early midline signalling in axial patterning of the eyes during development.

CONCLUSIONS

Taken together, our data show that global neurogenesis, patterning, and differentiation processes are relatively surprisingly "correct" in the CF neural retina. If the developmental program is correctly followed in the CF eye, then why do cells die, and why does the retina degenerate? The major difference between SF and CF developing eyes is their relative size, and the origin of this difference probably is to be found at neural plate stage, when increased midline signalling in CF reduces the eye field size (Strickler et al., 2001; Yamamoto et al., 2004). On the other hand, we have detected important cell death inside the neural retina with live LysoTracker experiments. This happens precisely a few hours after the lens enters into apoptosis. It is thus tempting to speculate that CF retina cells die as a consequence of defective signalling from the dying lens. The next step in understanding CF eye degeneration will clearly involve the analysis of lens-to-retina communication and of the initial trigger for lens apoptosis. The time course and anatomical analyses performed in the present study suggest that the origin of eye degeneration in CF should be discovered at very early stages of signalling and patterning of the neural plate.

ACKNOWLEGMENTS

We sincerely thank Laurent Legendre and Matthieu Simion for their invaluable help and advice in taking care of the *Astyanax* and Jean-Stéphane Joly for continuous support and interest. A.A., A.M., and E.C. are postdoctoral fellows supported by INRA, CNRS, and the European community, respectively.

LITERATURE CITED

Ando H, Kobayashi M, Tsubokawa T, Uyemura K, Furuta T, Okamoto H. 2005. *Lhx2* mediates the activity of *Six3* in zebrafish forebrain growth. Dev Biol 287:456–468.

Barbieri AM, Lupo G, Bulfone A, Andreazzoli M, Mariani M, Fougerousse F, Consalez GG, Borsani G, Beckmann JS, Barsacchi G, Ballabio A, Banfi S. 1999. A homeobox gene, *vax2*, controls the patterning of the eye dorsoventral axis. Proc Natl Acad Sci U S A 96:10729–10734.

Behrens M, Langecker TG, Wilkens H, Schmale H. 1997. Comparative analysis of *Pax-6* sequence and expression in the eye development of the blind cave fish *Astyanax fasciatus* and its epigean conspecific. Mol Biol Evol 14:299–308.

Borowsky R, Wilkens H. 2002. Mapping a cave fish genome: polygenic systems and regressive evolution. J Hered 93:19–21.

Candal E, Anadon R, DeGrip WJ, Rodriguez-Moldes I. 2005. Patterns of cell proliferation and cell death in the developing retina and optic tectum of the brown trout. Brain Res Dev Brain Res 154:101–119.

Cheng CW, Yan CH, Hui CC, Strahle U, Cheng SH. 2006. The homeobox gene *irx1a* is required for the propagation of the neurogenic waves in the zebrafish retina. Mech Dev 123:252–263.

Deyts C, Candal E, Joly JS, Bourrat F. 2005. An automated in situ hybridization screen in the medaka to identify unknown neural genes. Dev Dyn 234:698–708.

Esteve P, Bovolenta P. 2006. Secreted inducers in vertebrate eye development: more functions for old morphogens. Curr Opin Neurobiol 16:13–19.

Faillace MP, Julian D, Korenbrot JI. 2002. Mitotic activation of proliferative cells in the inner nuclear layer of the mature fish retina: regulatory signals and molecular markers. J Comp Neurol 451:127–141.

Fisher AJ, Reh TA. 2000. Identification of a proliferating marginal zone of retinal progenitors in postnatal chicken. Dev Biol 220:197–210.

Goodhill GJ, Richards LJ. 1999. Retinotectal maps: molecules, models and misplaced data. Trends Neurosci 22:529–534.

Harris WA, Perron M. 1998. Molecular recapitulation: the growth of the vertebrate retina. Int J Dev Biol 42:299–304.

Hooven TA, Yamamoto Y, Jeffery WR. 2004. Blind cavefish and heat shock protein chaperones: a novel role for hsp90alpha in lens apoptosis. Int J Dev Biol 48:731–738.

Jeffery WR. 2001. Cavefish as a model system in evolutionary developmental biology. Dev Biol 231:1–12.

Jeffery WR, Martasian DP. 1998. Evolution of eye regression in the cavefish *Astyanax*: apoptosis and the *Pax6* gene. Am Zool 38:685–696.

Jeffery WR, Strickler A, Guiney S, Heyser D, Tomarev S. 2000. *Prox1* in eye degeneration and sensory organ compensation during development and evolution of the cavefish *Astyanax*. Dev Genes Evol 210:223–230.

Kay JN, Roeser T, Mumm JS, Godinho L, Mrejeru A, Wong RO, Baier H. 2004. Transient requirement for ganglion cells during assembly of retinal synaptic layers. Development 131:1331–1342.

Kimmel CB, Ballard WW, Kimmel SR, Ullmann B, Schilling TF. 1995 Stages of embryonic development of the zebrafish. Dev Dyn 203:253–310.

Koshiba-Takeuchi K, Takeuchi JK, Matsumoto K, Momose T, Uno K, Hoepker V, Ogura K, Takahashi N, Nakamura H, Yasuda K, Ogura T. 2000. *Tbx5* and the retinotectum projection. Science 287:134–137.

Langecker TG, Schmale H, Wilkens H. 1993 Transcription of the opsin gene in degenerate eyes of cave dwelling *Astyanax fasciatus* (Teleostei, Characidae) and its conspecific ancestor during early ontogeny. Cell Tissue Res 273:183–192.

Lemke G, Reber M. 2005. Retinotectal mapping: new insights from molecular genetics. Annu Rev Cell Dev Biol 21:551–580.

Levine EM, Roelink H, Turner J, Reh TA. 1997. Sonic hedgehog promotes rod photoreceptor differentiation in mammalian retinal cells in vitro. J Neurosci 17:6277–6288.

Lupo G, Liu Y, Qiu R, Chandraratna RA, Barsacchi G, He RQ, Harris WA. 2005. Dorsoventral patterning of the *Xenopus* eye: a collaboration of retinoid, Hedgehog and FGF receptor signaling. Development 132: 1737–1748.

Marc RE, Cameron D. 2001. A molecular phenotype atlas of the zebrafish retina. J Neurocytol 30:593–654.

Marcus RC, Delaney CL, Easter SS Jr. 1999. Neurogenesis in the visual system of embryonic and adult zebrafish (*Danio rerio*). Vis Neurosci 16:417–424.

Martinez-Morales JR, Del Bene F, Nica G, Hammerschmidt M, Bovolenta P, Wittbrodt J. 2005. Differentiation of the vertebrate retina is coordinated by an FGF signaling center. Dev Cell 8:565–574.

Menuet A, Alunni A, Joly JS, Jeffery WR, Rétaux S. 2007 Expanded expression of Sonic Hedgehog in *Astyanax* cavefish: multiple consequences on forebrain development and evolution. Development 134: 845–855.

Mitchell RW, Russell WH, Elliott WR. 1971. Mexican eyeless characin fishes, genus *Astyanax*: environment, distribution, and evolution. Spec Publ Mus Texas Tech Univ 12:1–89.

Moshiri A, McGuire CR, Reh TA. 2005. Sonic hedgehog regulates proliferation of the retinal ciliary marginal zone in posthatch chicks. Dev Dyn 233:66–75.

Mui SH, Kim JW, Lemke G, Bertuzzi S. 2005. *Vax* genes ventralize the embryonic eye. Genes Dev 19:1249–1259.

Neumann CJ, Nuesslein-Volhard C. 2000. Patterning of the zebrafish retina by a wave of sonic hedgehog activity. Science 289:2137–2139.

Nguyen V, Joly J, Bourrat F. 2001. An in situ screen for genes controlling cell proliferation in the optic tectum of the medaka (*Oryzias latipes*). Mech Dev 107:55–67.

Perron M, Harris WA. 2000. Retinal stem cells in vertebrates. Bioessays 22:685–688.

Picker A, Brand M. 2005. Fgf signals from a novel signaling center determine axial patterning of the prospective neural retina. Development 132:4951–4962.

Porter FD, Drago J, Xu Y, Cheema SS, Wassif C, Huang SP, Lee E, Grinberg A, Massalas JS, Bodine D, Alt F, Westphal H. 1997. *Lhx2*, a LIM homeobox gene, is required for eye, forebrain, and definitive erythrocyte development. Development 124:2935–2944.

Reh TA, Fischer AJ. 2001. Stem cells in the vertebrate retina. Brain Behav Evol 58:296–305.

Retaux S, Harris WA. 1996. Engrailed and retinotectal topography. Trends Neurosci 19:542–546.

Reza HM, Yasuda K. 2004. Lens differentiation and crystallin regulation: a chick model. Int J Dev Biol 48:805–817.

Sasagawa S, Takabatake T, Takabatake Y, Muramatsu T, Takeshima K. 2002. Axes establishment during eye morphogenesis in *Xenopus* by coordinate and antagonistic actions of BMP4, Shh, and RA. Genesis 33:86–96.

Schaefer KS, Doughman YQ, Fisher SA, Watanabe M. 2004. Dynamic patterns of apoptosis in the developing chicken heart. Dev Dyn 229: 489–499.

Schulte D, Furukawa T, Peters MA, Kozak CA, Cepko CL. 1999. Misexpression of the *Emx*-related homeobox genes *cVax* and *mVax2* ventralizes the retina and perturbs the retinotectal map. Neuron 24:541–553.

Seth A, Culverwell J, Walkowicz M, Toro S, Rick JM, Neuhauss SC, Varga ZM, Karlstrom RO. 2006. *belladonna/(lhx2)* Is required for neural patterning and midline axon guidance in the zebrafish forebrain. Development 133:725–735.

Shkumatava A, Neumann CJ. 2005. Shh directs cell-cycle exit by activating p57Kip2 in the zebrafish retina. EMBO Rep 6:563–569.

Shkumatava A, Fischer S, Muller F, Strahle U, Neumann CJ. 2004. Sonic hedgehog, secreted by amacrine cells, acts as a short-range signal to direct differentiation and lamination in the zebrafish retina. Development 131:3849–3858.

Soares D, Yamamoto Y, Strickler AG, Jeffery WR. 2004. The lens has a specific influence on optic nerve and tectum development in the blind cavefish *Astyanax*. Dev Neurosci 26:308–317.

Stenkamp DL, Frey RA, Prabhudesai SN, Raymond PA. 2000. Function for Hedgehog genes in zebrafish retinal development. Dev Biol 220:238–252.

Strickler AG, Yamamoto Y, Jeffery WR. 2001. Early and late changes in *Pax6* expression accompany eye degeneration during cavefish development. Dev Genes Evol 211:138–144.

Strickler AG, Famuditimi K, Jeffery WR. 2002. Retinal homeobox genes and the role of cell proliferation in cavefish eye degeneration. Int J Dev Biol 46:285–294.

Take-uchi M, Clarke JD, Wilson SW. 2003. Hedgehog signalling maintains the optic stalk-retinal interface through the regulation of *Vax* gene activity. Development 130:955–968.

Voneida TJ, Sligar CM. 1976. A comparative neuroanatomic study of retinal projections in two fishes: *Astyanax hubbsi* (the blind cave fish), and *Astyanax mexicanus*. J Comp Neurol 165:89–105.

Wang Y, Dakubo GD, Thurig S, Mazerolle CJ, Wallace VA. 2005. Retinal ganglion cell-derived sonic hedgehog locally controls proliferation and the timing of RGC development in the embryonic mouse retina. Development 132:5103–5113.

Watanabe M, Hitomi M, van der Wee K, Rothenberg F, Fisher SA, Zucker R, Svoboda KKH, Goldsmith EC, Heiskanen KM, Nieminen AL. 2002. The pros and cons of apoptosis assays for use in the study of cells, tissues, and organs. Microsc Microanal 8:375–391.

Yamamoto Y, Jeffery WR. 2000. Central role for the lens in cave fish eye degeneration. Science 289:631–633.

Yamamoto Y, Stock DW, Jeffery WR. 2004. Hedgehog signalling controls eye degeneration in blind cavefish. Nature 431:844–847.

Yazulla S, Studholme KM. 2001. Neurochemical anatomy of the zebrafish retina as determined by immunocytochemistry. J Neurocytol 30:551–592.

Zuber ME, Gestri G, Viczian AS, Barsacchi G, Harris WA. 2003. Specification of the vertebrate eye by a network of eye field transcription factors. Development 130:5155–5167.